

Synthesis and Hierarchical Self-Assembly of Rod–Rod Block Copolymers via Click Chemistry between Mesogen-Jacketed Liquid Crystalline Polymers and Helical Polypeptides

Qing-Han Zhou, Ju-Kuan Zheng, Zhihao Shen,* Xing-He Fan,* Xiao-Fang Chen, and Qi-Feng Zhou*

Beijing National Laboratory for Molecular Sciences, Key Laboratory of Polymer Chemistry and Physics of Ministry of Education, College of Chemistry and Molecular Engineering, Peking University, Beijing 100871, China

Received April 6, 2010; Revised Manuscript Received June 1, 2010

ABSTRACT: A series of novel rod–rod diblock copolymers containing poly{2,5-bis[(4-methoxyphenyl)oxycarbonyl]styrene} (PMPCS) and poly(γ -benzyl-L-glutamate) (PBLG) were synthesized by click chemistry from alkyne- and azide-functionalized homopolymers. The α -alkyne PMPCS homopolymers were synthesized by copper-mediated atom transfer radical polymerization with a bromine-containing α -alkyne bifunctional initiator, and α -azido PBLG homopolymers were synthesized by ring-opening polymerization of γ -benzyl-L-glutamate *N*-carboxyanhydride with an amino-containing α -azide initiator. The molecular structures of the rod–rod block copolymers were confirmed by ^1H NMR spectroscopy, Fourier transform infrared spectroscopy, and gel permeation chromatography analysis. The self-assembling behavior of the rod–rod block copolymers in bulk was investigated using differential scanning calorimetry, polarized light microscopy, wide-angle X-ray diffraction, and transmission electron microscopy techniques. A lamellar structure was observed with f_{PBLG} of ~ 0.50 , in which PMPCS was in a columnar nematic phase and PBLG assigned to a hexagonally packed-cylinder structure (Φ_{H}). According to the TEM micrographs and simulated lengths of the copolymers, a stacked bilayer structure in a hexagon in lamella morphology for the self-assembly of the rod–rod block copolymers was proposed. Finally, by increasing f_{PBLG} to ~ 0.69 , a microphase-separated hexagon in cylinder morphology was found, in which PMPCS formed the core of the cylinders surrounded by PBLG in Φ_{H} phase and both rods were in an interdigitated packing.

Introduction

Block copolymers (BCPs) have attracted tremendous attention for their self-assembling properties in bulk or in selective solvents, forming various periodic patterns on the nanometer scale due to microphase separation.^{1–3} These morphologies, such as lamellae, cylinders, gyroids, and spheres, are determined by the volume fraction of one component f , the total degree of polymerization N of the block copolymer, and the Flory–Huggins interaction parameter χ . Coil–coil block copolymers have already gained an enormous interest from scientists since a couple of decades ago and have been practically used as materials in nowadays life attributed to the successful establishment of their experimental and theoretical phase diagrams.^{2–4} Compared with coil–coil diblock copolymers, for rod–coil BCPs, the aggregation between rigid-rod blocks and high Flory–Huggins interaction parameter χ can allow microphase separation to occur at relatively low degrees of polymerization and at a rather short length of a few nanometers.^{5–7} Unique and nonpredicted morphologies from rod–coil BCPs have been found, which have been widely investigated and reviewed during the past decade.^{8–10} In contrast, the synthesis and self-assembly of rod–rod block copolymers is still a relatively new research area; however, it promises real-world applications, such as biosensors, scaffolds for tissue engineering, heterojunction solar cells, and photodetectors.^{11,12} Accordingly,

researches into rod–rod BCPs have been greatly intensified during recent years.

Generally, for rod–rod BCPs, due to the rigid nature and higher persistence length of each block, low-curvatures aggregates, such as vesicles in selective solvents and lamellar structures in solid state, will be formed.¹³ Rod–rod block copolymers solely based on polypeptides have been already synthesized.^{14–16} Vesicular structures were observed in water by self-assembly of poly(leucine-*b*-poly(hydroxylated glutamate) copolymer which could mimic the assembly conformation of protein as a novel biomaterial in medical use.¹⁷ In addition, the so-called schizophrenic vesicles were found by zwitterionic diblock copolymer poly(L-glutamic acid)-*b*-poly(L-lysine),¹⁸ so were micelles by miktoarm star copolymers,¹⁹ which would likely find potential use in controlled drug delivery systems. Kros *et al.* synthesized polyisocyanide-*b*-poly(γ -benzyl-L-glutamate) diblock copolymers and observed vesicles with a diameter of $> 5 \mu\text{m}$ by using laser scanning confocal and optical microscopes.²⁰ Lamellar morphologies, including hexagon in lamella (HL) structure, in bulk were investigated for peptide-containing copolymers as well.^{21,22} Rod–rod BCPs containing polypeptide and π -conjugated polymer blocks were also studied, and samples showed different nanostructures depending on the block composition and the polypeptide secondary structure.²³

On the other hand, mesogen-jacketed liquid crystalline polymers (MJLCPs) represent a special class of liquid crystalline polymers (LCPs) which attracted increasing interest in recent years.^{24,25} In this kind of liquid crystalline polymers mesogenic

*To whom correspondence should be addressed. E-mail: (Z.S.) zshen@pku.edu.cn; (X.-H.F.) fanxh@pku.edu.cn; (Q.-F.Z.) qfzhou@pku.edu.cn.

pendants are considered to be densely packed around the backbone, and force the backbone to adopt a rigid or semirigid conformation.²⁶ Rod-like MJLCPs have good tunability in rod length, while the rod diameter can also be altered by varying the lengths of both the rigid core and flexible tails in the mesogenic side chains.²⁷ Because of the above properties, MJLCPs have been widely used as rod blocks in synthesizing well-defined rod-coil diblock and triblock copolymers.^{28–32} However, rod-rod diblock copolymers containing MJLCP building blocks have never been reported so far. Study on this kind of copolymers will greatly enrich the liquid crystalline and self-assembling behaviors of MJLCPs. On the other hand, polypeptides have shown charming properties for their self-assembling properties and potential real-world applications for decades.^{33–35} Therefore, we are specifically interested in the synthesis, self-assembly behavior, and potential applications of rod-rod diblock copolymers containing both MJLCPs and polypeptides.

Recently, we have designed and obtained a new kind of rod-rod diblock copolymer poly{2,5-bis[4-methoxyphenyl]oxycarbonylstyrene}-*b*-poly(γ -benzyl-L-glutamate) (PMPCS-*b*-PBLG). In this contribution, we describe here the synthesis of these block copolymers by combining atom transfer radical polymerization (ATRP) of 2,5-bis[4-methoxyphenyl]oxycarbonylstyrene, ring-opening polymerization (ROP) of γ -benzyl-L-glutamate *N*-carboxyanhydride, and a subsequent copper-catalyzed click chemistry to form a series of rod-rod BCPs with different volume fractions of the two blocks. The phase behavior of the rod-rod BCPs with different volume fractions were investigated in this study, and hierarchical self-assembling structures on nanometer scale were analyzed by differential scanning calorimetry (DSC), polarized light microscopy (PLM), wide-angle X-ray diffraction (WAXD), and transmission electron microscopy (TEM) techniques. To the best of our knowledge, this is the first example of utilizing a facile and efficient click coupling reaction to prepare rod-rod diblock copolymers containing an α -helical polypeptide and a rigid vinylic polymer, although syntheses of rod-coil BCPs by click chemistry have been reported in literature.^{36,37}

Experimental Section

Materials. 2-Bromo-2-methylpropionyl bromide (98%, Acros), 3-chloropropylamine hydrochloride (98%, Acros), propargyl alcohol (99%, Aldrich), sodium azide (99%), *N,N,N',N''*-pentamethyl diethylenetriamine (PMDETA) (98%, TCI), and triethylamine (98%) were used as received. *N,N*-Dimethylformamide (DMF) and tetrahydrofuran (THF) (Beijing Chemical Reagents Co., A.R. grade) were used after distilled. Chlorobenzene was purified by washing with concentrated sulfuric acid to remove residual thiophenes, followed by washing with a 5% sodium carbonate solution, and again with water, then dried with anhydrous calcium chloride and finally distilled.

Synthesis of α -Functionalized Initiators. Synthesis of Propargyl 2-Bromoisobutyrate. Propargyl alcohol (1.1 g, 19.6 mmol) and triethylamine (3.5 g, 23.5 mmol) were dissolved in methylene chloride (20 mL), and 2-bromo-2-methylpropionyl bromide (3.0 g, 23.5 mmol) was added dropwise slowly.

The reaction mixture was cooled in an ice-water bath, and was stirred at 0 °C for 30 min and then at room temperature for 4 h. The filtered solution was washed with water for three times, and distilled under vacuum. A purified product was easily obtained by passing through a silica gel column. Yield: 3.09 g (77%). ¹H NMR (CDCl₃): δ 4.78 (d, 2H, CH₂O), 2.53 (t, 1H, C \equiv CH), and 1.96 (s, 6H, (CH₃)₂C).

Synthesis of 1-Azido-3-aminopropane. This compound was synthesized following an already published procedure.³⁸ A solution of 3-chloropropylamine hydrochloride (2 g, 15.4 mmol) and sodium azide (3.8 g, 58.5 mmol) in water (20 mL) was heated at 80 °C for 15 h. After water was almost removed by distillation under vacuum, the reaction mixture was cooled in an ice-water

bath. Methylene chloride (50 mL) and KOH (2.2 g) were added, with the temperature remaining under 10 °C while being stirred. After filtration, the aqueous phase was extracted with diethyl ether three times. The combined organic layers were dried with Mg₂SO₄ and concentrated to afford an oil by distillation. Yield: 1.2 g (78%). ¹H NMR (CDCl₃): δ 3.38 (t, 2H, CH₂N₃), 2.81 (t, 2H, CH₂NH₂), 1.73 (q, 2H, CH₂CH₂CH₂), and 1.17 (s, 2H, NH₂).

Polymerization Reactions. Synthesis of α -Alkyne PMPCS. The monomer of PMPCS, {2,5-bis[4-methoxyphenyl]oxycarbonylstyrene} (MPCS), was prepared as described in the literature.³⁹ In a typical experiment for polymerization, MPCS (0.202 g, 50 μ mol), propargyl 2-bromoisobutyrate (2.05 mg, 10 μ mol), CuBr (1.43 mg, 10 μ mol), PMDETA (1.73 mg, 10 μ mol), and chlorobenzene (2.02 mL) were charged into a polymerization tube under ambient atmosphere. After stirred and degassed by three freeze-thaw cycles, the tube was sealed under vacuum. Subsequently, the tube was immersed into a thermostated oil bath at 90 °C for 12 h, and then quenched in cold THF to room temperature. The solution was passed through a neutral alumina column in order to remove copper salt. The polymer was precipitated in a large volume of methanol, and dried in a vacuum overnight.

Synthesis of α -Azido PBLG. γ -Benzyl-L-glutamate *N*-carboxyanhydride (Bz-L-GluNCA) was prepared according to a literature procedure.⁴⁰ In a typical experiment, Bz-L-GluNCA (0.789 g, 3.0 mmol), 1-azido-3-aminopropane (3.0 mg, 30 μ mol), and 2.63 mL of anhydrous DMF were introduced into a dry Schlenk flask. After degassed by three freeze-thaw cycles, the solution was stirred for 3 days at room temperature under Ar atmosphere. The polymer was precipitated in diethyl ether and dried under vacuum.

Synthesis of PMPCS-*b*-PBLG Block Copolymers by Huisgen's 1, 3-Dipolar Cycloaddition. Typically, α -alkyne PMPCS (0.168 g, 24 μ mol, 1.2 equiv), α -azido PBLG (0.216 g, 20 μ mol, 1 equiv), and PMDETA (6.93 mg, 40 μ mol, 2 equiv) were introduced into a Schlenk flask in 2 mL anhydrous DMF. After degassed by one freeze-thaw cycle, CuBr (5.74 mg, 40 μ mol, 2 equiv) was added rapidly. The Schlenk flask was immersed into a thermostated oil bath at 35 °C for 24 h. The reaction mixture was passed through a neutral alumina column in order to remove copper salt, and precipitated in excess of diethyl ether. The product was filtered and washed with a mixed solvent of methanol and acetone to remove excess of PMPCS. Table 1 summarized the molecular characteristics of the homopolymers and diblock copolymers presented in this work.

Characterization. The molar masses were determined with the combination of gel permeation chromatography (GPC), ¹H NMR, and matrix-assisted laser desorption/ionization time-of-flight mass spectrometry (MALDI-TOF MS) measurements. GPC experiments were conducted on a Waters 2410 instrument equipped with a Waters 2410 RI detector and two Waters μ -Styragel columns (103, 104 Å), with THF or DMF as eluent (1.0 mL/min) in presence of LiBr (1 g/L). The calibration curve was obtained with linear polystyrenes as standards. ¹H NMR spectra were obtained with a Bruker 400 MHz spectrometer. MALDI-TOF MS measurements were performed on a Bruker Autoflex high-resolution tandem mass spectrometer. Thermogravimetric analysis (TGA) was performed on a TA Q600 SDT instrument in nitrogen atmosphere. DSC examination was carried out on a TA Q100 DSC calorimeter in nitrogen atmosphere. PLM observation was performed on a Nikon DS-Ri1 microscope with an Instec HCS302 hot stage. One-dimensional (1D) WAXD experiments were carried out on a Philips X'Pert Pro diffractometer with a 3 kW ceramic tube as the X-ray source (Cu K α) and an X'celerator detector. Two-dimensional (2D) WAXD patterns were obtained using a Bruker D8Discover diffractometer with a GADDS as a 2D detector calibrated with silicon powder and silver behenate. The oriented films by mechanical shearing were mounted on the sample stage with the

point-focused X-ray incident beam either parallel (X direction) or perpendicular (Y or Z direction) to the shear direction (X direction). The background scattering was recorded and subtracted from the sample patterns. TEM was used to investigate

Table 1. Molecular Characteristics of α -Functionalized PMPCS and PBLG Homopolymers and PMPCS- b -PBLG Block Copolymers

sample	M_n (g/mol)	DP_n^c	PDI^d	f_{PBLG}^e (%)
alkyne-PMPCS ₄₂	17 300 ^a	42	1.16	
azido-PBLG ₁₉	4 300 ^b	19	1.26	
azido-PBLG ₄₉	10 900 ^b	49	1.28	
azido-PBLG ₈₀	17 700 ^b	80	1.27	
azido-PBLG ₁₁₂	24 700 ^b	112	1.25	
azido-PBLG ₁₇₃	38 200 ^b	173	1.25	
PMPCS ₄₂ - b -PBLG ₁₉	21 600 ^b	-	1.28	20
PMPCS ₄₂ - b -PBLG ₄₉	28 200 ^b	-	1.31	38
PMPCS ₄₂ - b -PBLG ₈₀	35 000 ^b	-	1.28	50
PMPCS ₄₂ - b -PBLG ₁₁₂	42 000 ^b	-	1.33	58
PMPCS ₄₂ - b -PBLG ₁₇₃	55 500 ^b	-	1.33	69

^a M_n value determined by GPC in THF (calibrated with polystyrene standards) is 11 400 g/mol. However, a PMPCS sample with an M_n (GPC) value of 6 050 g/mol is found to have an absolute molecular weight of 9 220 g/mol by using MALDI-TOF MS, which leads to a factor of 1.52 between these two molecular weights. Assuming that the shape of PMPCS does not change dramatically, the molecular weight of alkyne-PMPCS₄₂ should be 17 300 g/mol (11 400 g/mol \times 1.52). ^b The molecular weights of the copolymers and their corresponding PBLG blocks were calculated from the M_n of alkyne-PMPCS₄₂ and the area ratio of characteristic resonance (methyl group) of PMPCS to that (methylene group of benzyl) of the PBLG block in ¹H NMR spectra. ^c Degree of polymerization of homopolymers. ^d Determined by GPC in DMF in presence of LiBr at 1 g/L. ^e Volume fraction of PBLG; calculated using the number-average degrees of polymerization of the PMPCS segment and the PBLG block in combination with the following densities: PMPCS, $\rho = 1.26$ g/cm³; ⁴¹ PBLG, $\rho = 1.28$ g/cm³. ⁴²

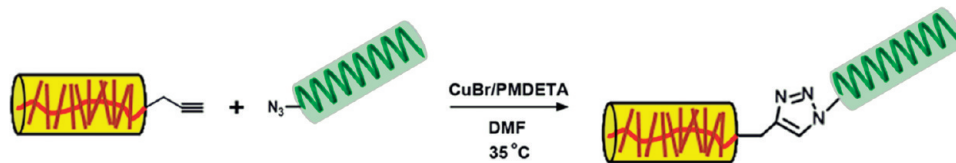
the microphase separation of samples on a Hitachi H-800 electron microscope. The solution-cast and ultramicrotomed sample films were stained by RuO₄ vapor to enhance contrast.

Results and Discussion

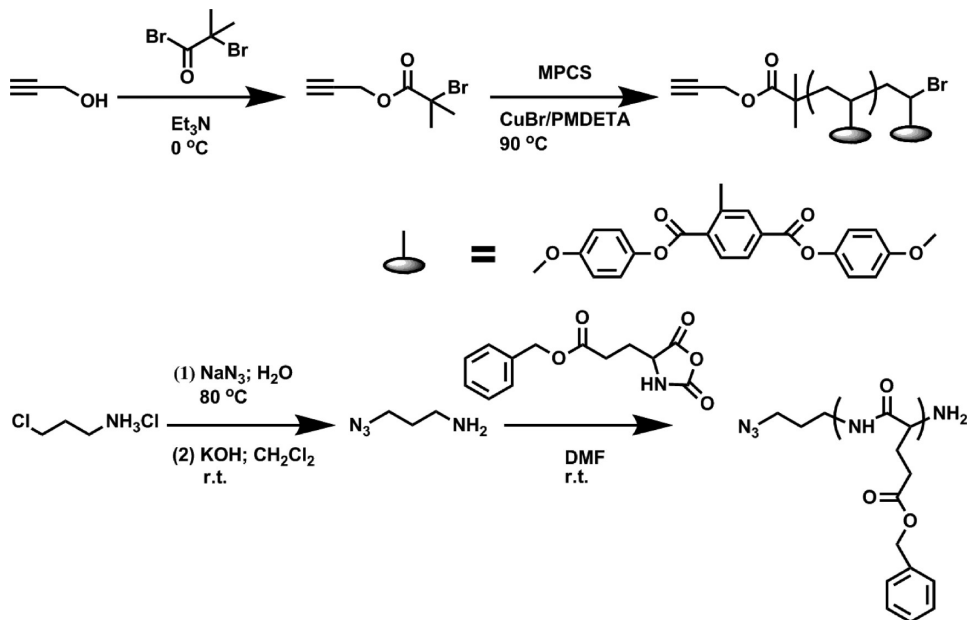
Synthesis of PMPCS- b -PBLG Rod-Rod Diblock Copolymers by Click Chemistry from Homopolymers. The synthesis of rod-rod diblock copolymers is outlined in Schemes 1 and 2, which was started with the preparation of α -alkyne-terminated PMPCS by copper-mediated atom transfer radical polymerization and that of α -azide-functionalized PBLG by ring-opening polymerization of Bz-L-GluNCA, followed by Huisgen's 1,3-dipolar cycloaddition (click chemistry) to connect the two rigid-rod blocks. The α -alkyne initiator was prepared by commercially available reagents, 2-bromo-2-methylpropionyl bromide and propargyl alcohol, according to published procedure.⁴³ The α -alkyne initiator was used to trigger ATRP of MPCS in chlorobenzene, using copper bromide (CuBr) complexed by PMDETA, and the alkyne hydrogen did not interfere with the polymerization. The proton of alkyne-terminated homopolymer was clearly identified by ¹H NMR (shown in Figure 1a), and GPC analysis was utilized to confirm the α -functionalized PMPCS precursor as well. Figure 1a shows the ¹H NMR spectrum of alkyne-PMPCS₄₂ in CDCl₃. The resonance signals of protons of trisubstituted phenyl (f, g, and h), disubstituted phenyl (i and j), methyl group (k), and vinyl backbone (d and e) appeared at $\delta = 7.2$ –8.0, 6.4–7.0, 3.4–3.9, and 1.6–1.9 ppm, respectively. Signals of alkyne (a) and methylene (b) protons related to the initiator appeared at $\delta = 2.2$ and 3.9 ppm, respectively.

It is well-known that primary amine residues can be employed for the ROP of α -amino acid N -carboxyanhydride.³⁸

Scheme 1. Synthesis of PMPCS- b -PBLG Diblock Copolymers by Click Chemistry



Scheme 2. Synthetic Pathway to α -Functionalized Homopolymers



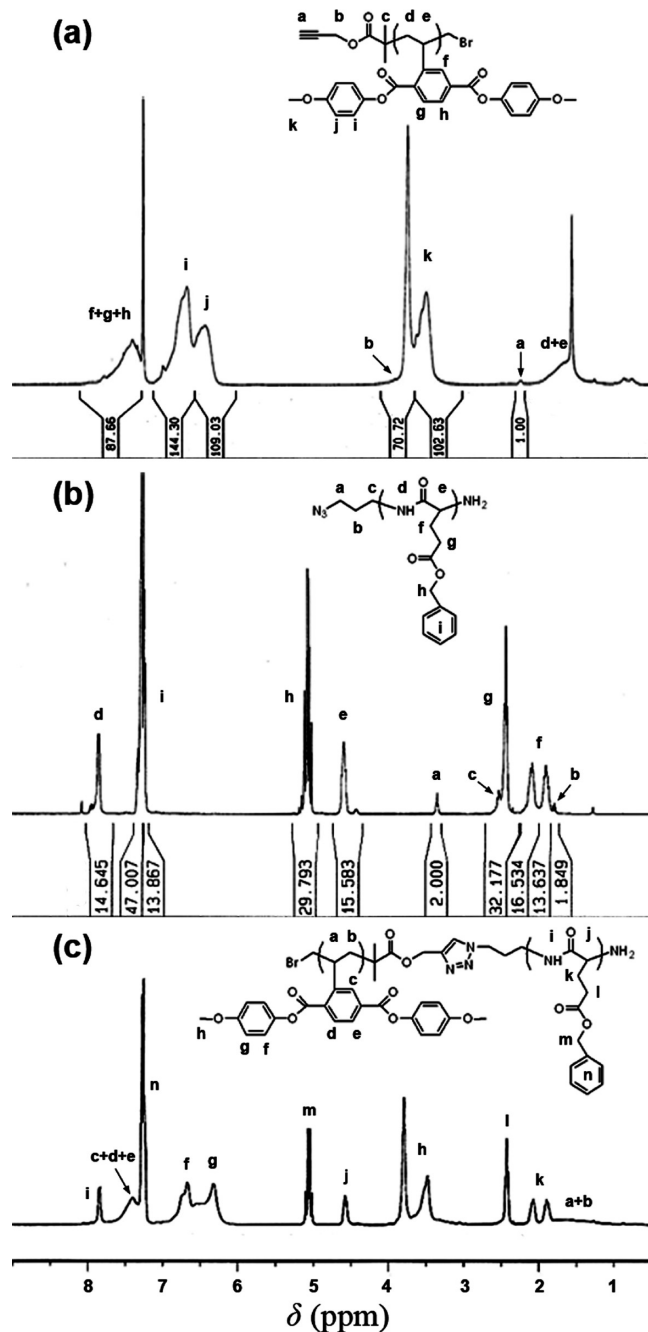


Figure 1. ¹H NMR spectra of alkyne-PMPCS₄₂ (a), azido-PBLG₁₉ (b), and PMPCS₄₂-b-PBLG₁₉ (c) in a CDCl₃/TFA mixture with 15% TFA.

In the present work, 1-azido-3-aminopropane was used to facilitate the polymerization of polypeptide from Bz-L-GluNCA. GPC analysis in DMF verified the synthesis of the homopolymer, in which LiBr was added to minimize polymer aggregation. The azido-functional group of the PBLG precursor was clearly evidenced by ¹H NMR in CDCl₃ with 15% trifluoroacetic acid (TFA). In Figure 1b, the resonance signals of protons of amide group (d), phenyl group (i), methylene group of benzyl (h), α-methine group (e), and β- and γ-methylene groups (g and f) appeared at δ = 7.9, 7.2–7.3, 5.1, 4.6, and 1.9–2.5 ppm, respectively. The signals of α-, β-, and γ-methylene protons (a, b, and c) adjacent to the azide group were observed at δ = 3.35, 1.85, and 2.53 ppm, respectively.

The following was the “click chemistry” between the azido-PBLG and the alkyne-PMPCS. The 1,3-dipolar cycloaddition coupling reaction was performed in DMF at

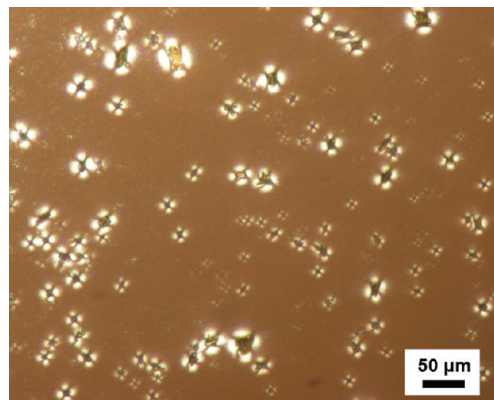


Figure 2. Representative texture of PMPCS₄₂-b-PBLG₁₉ at 135 °C from PLM observation.

35 °C using CuBr complexed by PMDETA in a Schlenk flask.⁴⁴ GPC measurements in DMF (LiBr, 1 g/L) and ¹H NMR experiments (CDCl₃/TFA with 15% TFA) were carried out to verify the completion of the coupling reaction. The corresponding resonance signals of protons in each block are shown in Figure 1c. Moreover, FTIR was also used to monitor the azide vibrational band for the completion of the click coupling reaction. The FTIR spectrum of azido-PBLG clearly revealed the presence of the vibrational band at 2098 cm⁻¹, which was characteristic of azide moieties (Figure S1 in Supporting Information, see spectrum of azido-PBLG₁₉ as an example), and the disappearance of the azide band in the spectra of the copolymers evidenced the completion of the coupling reactions. On the other hand, the amide I and amide II bands at 1655 and 1550 cm⁻¹ are characteristic of the peptidic α-helical secondary structure.⁴⁵ For polypeptides possessing a β-sheet conformation, position of the amide I band for parallel β-sheet is in the range of 1636–1640 cm⁻¹, and for the antiparallel β-sheet in the range of 1622–1632 cm⁻¹.⁴⁶ In the spectra of the copolymers, amide I bands around 1655 cm⁻¹ and the increase in the absorbance of the amide II bands at 1550 cm⁻¹ were distinctively observed for the copolymers with increasing content of PBLG, in which the PBLG block had an α-helical conformation as indicated by the FTIR spectra. For the sample of azido-PBLG₁₉, a shoulder band at 1625 cm⁻¹ was also observed in the FTIR spectrum, indicating that antiparallel β-sheet structure was in coexistence with the α-helical structure of PBLG with a low degree of polymerization.⁴⁷

Phase Structure and Self-Assembly in Bulk. DSC was used to study the thermal transitions of the diblock copolymers. Glass transitions were observed at ~15 °C for PBLG blocks and ~130 °C for PMPCS blocks during the first cooling and subsequent heating scans of the copolymers. PLM was used to observe birefringence of the copolymers. Sample films were cast from THF solutions by drying at room temperature. The liquid crystalline birefringence was observed at around 135 °C. The texture of PMPCS₄₂-b-PBLG₁₉ is shown in Figure 2 as an example. The birefringence did not disappear when the sample was heated to 190 °C, which was near the limit of thermal stability for PBLG, and subsequently cooled to room temperature, which implied that the samples formed their liquid crystalline phases at high temperatures (above 135 °C) and these phases remained unchanged upon cooling.

In order to account for the self-assembly of the copolymers, films with about 30 mg of samples were prepared from solution-casting for 1D WAXD experiments which were performed at different temperatures from 40 to 190 °C.

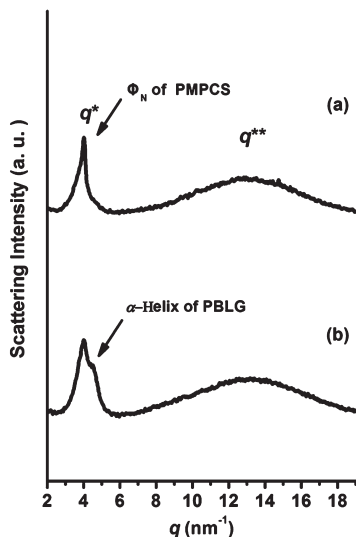


Figure 3. 1D WAXD patterns of PMPCS₄₂-*b*-PBLG₁₉ (a) and PMPCS₄₂-*b*-PBLG₄₉ (b) copolymers during the first heating at 170 °C.

Figure 3 shows the 1D WAXD patterns of PMPCS₄₂-*b*-PBLG₁₉ and PMPCS₄₂-*b*-PBLG₄₉. In the sample PMPCS₄₂-*b*-PBLG₁₉, one diffuse halo at larger q values ($q = 4\pi(\sin \theta)/\lambda$, where q is the scattering vector, θ the scattering angle in WAXD experiments, and λ the wavelength of X-ray) and a relatively sharp peak at lower q values were observed. The peak with q^* at 3.97 nm^{-1} (corresponding to a d -spacing of 1.58 nm) could be attributed to the columnar nematic phase (Φ_N) of PMPCS, while the diffuse halo with q^{**} at $\sim 13 \text{ nm}^{-1}$ (corresponding to a d -spacing of about 0.48 nm) was attributed to the distances between mesogens, polymer backbones, and other parts of the BCP.⁴⁸ The 1D WAXD pattern of PMPCS₄₂-*b*-PBLG₄₉ exhibited rather similar profile to that of PMPCS₄₂-*b*-PBLG₁₉ for the Φ_N phase of PMPCS with a d -spacing of 1.56 nm, and the reflection for PBLG was also found at 4.48 nm^{-1} with a d -spacing of 1.40 nm, which corresponded to a columnar diameter of 1.62 nm. The appearance of reflections from both PMPCS and PBLG indicated the microphase separation of the block copolymer. However, contrary to a well ordered, tight hexagonal columnar packing of polypeptides in α -helical conformation, absence of higher-order Bragg reflections in the WAXD pattern of PMPCS₄₂-*b*-PBLG₄₉ indicated that the PBLG helices were in a poorly ordered packing.^{47,49,50} A relatively low volume fraction of the PBLG block might be the reason for this point. Annealing at high temperatures was reported to help improve the level of ordering in some rod-coil systems.⁵¹ However, it worked little in this rod-rod system probably because of the rigid nature of each block. The microphase separation of the copolymers was investigated using TEM. However, no patterned structure was observed in both samples, which was possibly caused by the low composition of PBLG blocks and the poorly ordered PBLG helices for PMPCS₄₂-*b*-PBLG₁₉ and PMPCS₄₂-*b*-PBLG₄₉.

The phase transition and self-assembling behavior of samples PMPCS₄₂-*b*-PBLG₈₀ and PMPCS₄₂-*b*-PBLG₁₁₂ were also investigated. 1D WAXD was facilitated to investigate the phase behavior of samples at different temperatures from 40 to 170 °C (shown in Figure 4). Upon the first heating and cooling procedures, the Bragg reflections were found at scattering vectors with a ratio of $1:3^{1/2}:4^{1/2}:7^{1/2}$ for PMPCS₄₂-*b*-PBLG₈₀ at q of 4.60, 8.12, 9.43, and 12.17 nm^{-1} , and for PMPCS₄₂-*b*-PBLG₁₁₂ at q of 4.65, 8.13, 9.39, and 12.20 nm^{-1} , indicating the highly ordered hexagonal columnar

arrangement (Φ_H) of α -helical PBLG, and the Φ_H phase was developed upon first heating at about 130 °C.⁴⁷ It indicated that following the increase of volume fraction to $\sim 50\%$, the Φ_H phase was well developed, i.e., the structure of the PBLG blocks transformed from a poorly ordered hexagonal arrangement into an ordered one. The existence of such ordered packing of PBLG indicated the microphase separation of the block copolymers. The columnar diameters of PBLG helices for PMPCS₄₂-*b*-PBLG₈₀ and PMPCS₄₂-*b*-PBLG₁₁₂ were 1.58 and 1.56 nm, respectively. The decrease in the columnar diameter of the PBLG block indicated that the helices were packed into a more ordered hexagonal arrangement for longer PBLG due to the increasing hydrogen-bonding effect.⁴⁷ On the other hand, the peaks attributed to the Φ_N phase of PMPCS were partially embedded in the strong, first-order reflection of the Φ_H phase of PBLG in sample PMPCS₄₂-*b*-PBLG₁₁₂ due to the decrease in the volume fraction of PMPCS. The diffuse halo at 14 nm^{-1} with a corresponding d -spacing of 0.46 nm, which was a small decrease compared to 0.48 nm from the 1D WAXD patterns of PMPCS₄₂-*b*-PBLG₁₉ and PMPCS₄₂-*b*-PBLG₄₉, could be attributed to the increase in the amount of amorphous, smaller side chains of PBLG (compared to those of PMPCS). And the diameter of PMPCS columns was 1.56 nm for PMPCS₄₂-*b*-PBLG₁₁₂.

To further confirm the phase structure of the block copolymers, 2D WAXD experiments were carried out on mechanically sheared samples. Parts a and b of Figure 5 show the 2D WAXD patterns taken with the X-ray beam along Y and Z directions at room temperature, respectively. In Figure 5a, two pairs of strong diffraction arcs could be observed on the meridian in the low-angle region, which were attributed to the Φ_N phase of PMPCS and the Φ_H phase of PBLG, respectively. In Figure 5c, a set of Bragg reflections from the hexagonally ordered packing of PBLG at $q = 4.7, 8.3, 9.8,$ and 12.6 nm^{-1} was observed with a scattering vector ratio of $1:3^{1/2}:4^{1/2}:7^{1/2}$ in the integration at a 30° -angle centered at the meridian shown in Figure 5a, which was consistent with the 1D WAXD results. The columnar diameter of PBLG helices was 1.54 nm. In Figure 5d, only a pair of diffraction arcs could be observed on the meridian, in which the reflection from the Φ_N phase of PMPCS was embedded in the first-order reflection of the Φ_H phase of PBLG as mentioned above in the 1D WAXD results. The 2D WAXD results indicated that the long axes of the PMPCS and PBLG rods were both aligned parallel to the X direction and to the lamellar normal. In other words, the PMPCS rods were aligned parallel to the PBLG rods. For the 2D WAXD patterns of the sample of PMPCS₄₂-*b*-PBLG₁₁₂, a set of Bragg reflections from the hexagonally ordered packing of PBLG at $q = 4.8, 8.6, 10.1,$ and 12.7 nm^{-1} was also observed with a scattering vector ratio of $1:3^{1/2}:4^{1/2}:7^{1/2}$ in the integration at a 30° -angle centered at the meridian shown in Figure 5d, in which the columnar diameter of the PBLG hexagon was 1.52 nm from the data above (shown in Figure 5f).

The morphology of an alternating lamellar structure was observed by using TEM. Observations were performed on solution-cast films from solutions at a low concentration of 0.5 mg/mL. The film samples were stained by RuO₄ vapor to enhance contrast after annealing at 170 °C for 10 h. TEM micrographs revealed that the distances between lamellae of alternating PMPCS layer (dark parts) and PBLG layer (light parts) were about 49 nm for PMPCS₄₂-*b*-PBLG₈₀ and 58 nm for PMPCS₄₂-*b*-PBLG₁₁₂ (shown in Figure 6). The above results indicated that the formation of liquid crystalline (LC) phases did not destroy the microstructure regardless of the change in the diameter of the PMPCS or PBLG rod.⁵²

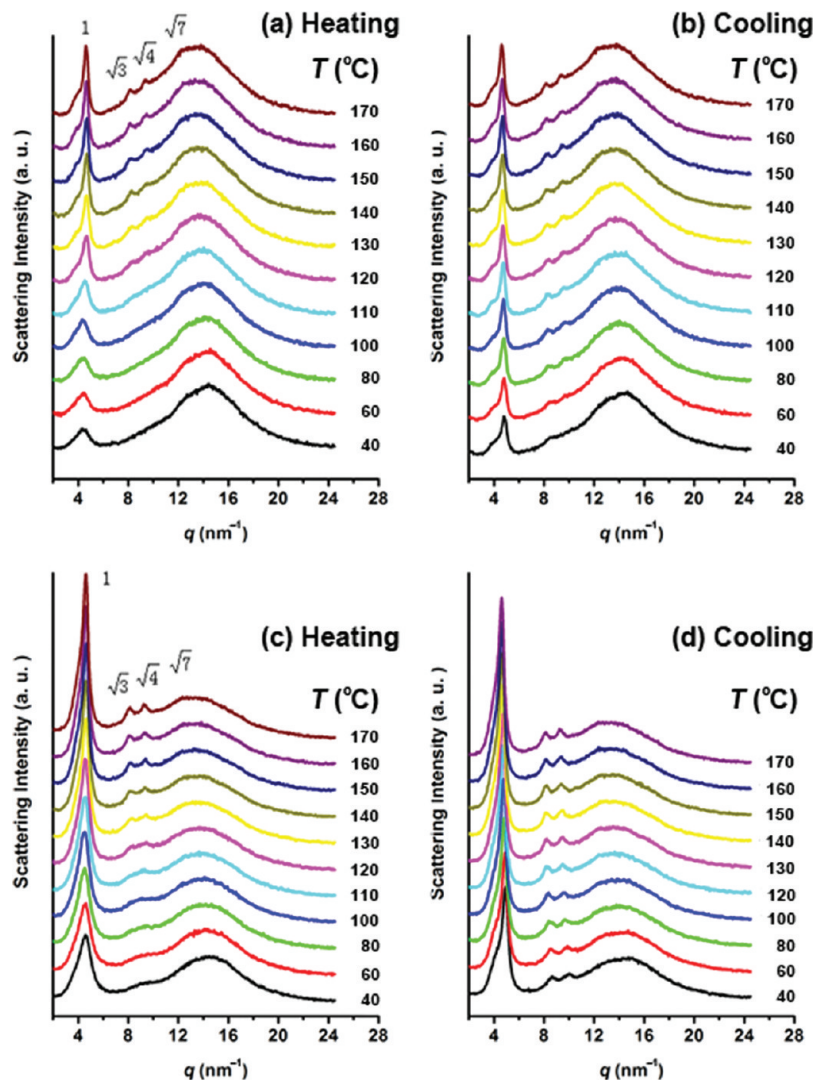


Figure 4. 1D WAXD powder patterns of samples PMPCS₄₂-*b*-PBLG₈₀ and PMPCS₄₂-*b*-PBLG₁₁₂ during the first heating (parts a and c, respectively) and first cooling (parts b and d, respectively).

However, the lamellar microstructures shown in the TEM micrographs were not well ordered, which was probably because the rigid rods had low chain mobility to form highly ordered patterns.

According to the above data from FTIR, 1D WAXD, and 2D WAXD experiments, the PBLG blocks could be assigned to a tightly packed hexagonal domain in the lamellar structure, and were considered to be packed next to the columnar nematic domain formed by the PMPCS blocks for sample PMPCS₄₂-*b*-PBLG₁₁₂. The proposed structure of the diblock copolymer is similar to the so-called HL or a cylinders-in-lamella morphology which has been reported on PBLG-*b*-polyglycine and PBLG-*b*-poly(L-lysine) peptide copolymers, and also in some other rod-coil systems.^{21,35,49} The PBLG segment had a hexagonal packing, with a columnar diameter of 1.56 nm for sample PMPCS₄₂-*b*-PBLG₁₁₂. Twice of the molecular lengths of the copolymers (47 nm for PMPCS₄₂-*b*-PBLG₈₀ and 56 nm for PMPCS₄₂-*b*-PBLG₁₁₂) on the basis of the molecular length simulation agreed well with the TEM observations, and the difference between the layer distances (about 9 nm) of the two samples was close to twice of the increase in length (4.8 nm × 2) of the PBLG block, in which the polypeptide segments adopted an 18/5 α -helical conformation and the PMPCS was presumed to have an extended chain conformation of the vinyl backbone. A bilayer structure appears more reasonable since the

interdigitated lamellar structure has a maximal layer distance less than 30 nm by simulation. Therefore, we propose a stacked bilayer structure in the HL morphology for the self-assembly of PMPCS₄₂-*b*-PBLG₈₀ and PMPCS₄₂-*b*-PBLG₁₁₂.

WAXD and TEM techniques were also used to investigate the self-assembling morphology of sample PMPCS₄₂-*b*-PBLG₁₇₃. In the 1D WAXD patterns (shown in Figure 7, parts a and b), upon the first heating and cooling procedures, the Bragg reflections were found at scattering vectors with a ratio of 1:3^{1/2}:4^{1/2} at 4.64, 8.06, and 9.25 nm⁻¹, indicating the hexagonal columnar arrangement (Φ_H) of α -helical conformation of PBLG with a columnar diameter of 1.56 nm, and the Φ_H phase of PBLG was developed upon first heating at about 140 °C. Again, the existence of such an ordered packing of PBLG indicated the microphase separation of the block copolymer. The peak attributed to the columnar nematic phase of PMPCS was difficult to observe because it was embedded in the strong, first-order reflection of the Φ_H phase of PBLG at a high f_{PBLG} . The cylinder morphology was found in the TEM micrographs on thin, ultramicrotomed films. RuO₄ vapor was used to stain the thin sample sections to enhance contrast after the sample was annealed at 130 °C for 3 days and sheared. Layer-like structures formed by alternating dark (PMPCS) and light (PBLG) strips were clearly observed in Figure 7c, and the average

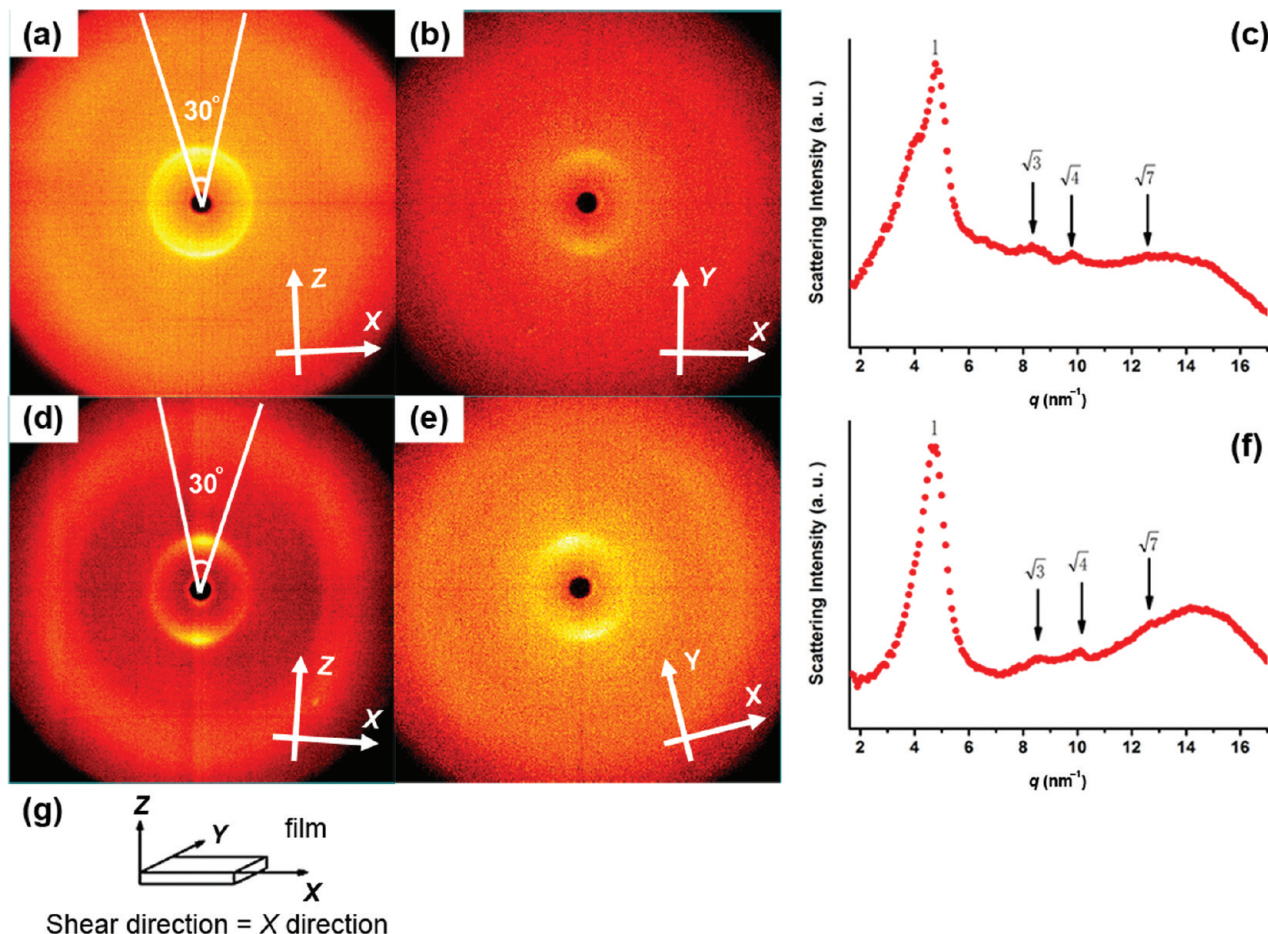


Figure 5. 2D WAXD patterns of sheared film samples of PMPCS₄₂-*b*-PBLG₈₀ (a and b) and PMPCS₄₂-*b*-PBLG₁₁₂ (d and e) with X-ray incident beam along *Y* and *Z* directions, respectively. Integration at a 30°-angle centered at the meridian shown in parts a (c) and d (f). Schematic drawing of the shearing geometry with *X*-axis the shear direction (g).

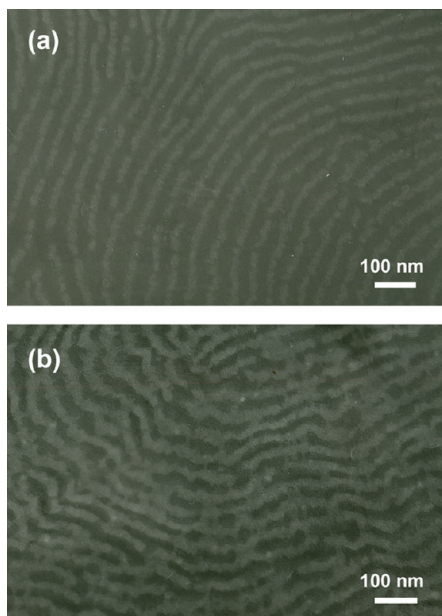


Figure 6. TEM micrographs of PMPCS₄₂-*b*-PBLG₈₀ (a) and PMPCS₄₂-*b*-PBLG₁₁₂ (b) stained by RuO₄ after 10-h annealing at 170 °C.

distance between layers was about 38 nm estimated from this figure. In Figure 7d, the dark circles were packed within the

PBLG (light) matrix, and an average circle-to-circle distance of about 42 nm could be estimated from this figure. The TEM results indicated a cylinder morphology with the PMPCS domain as cylinders and PBLG domain as the matrix. The simulated molecular length of the copolymer (about 37 nm) was consistent with the estimated distance between the PMPCS cylinders from the TEM micrographs, which indicated that PMPCS and PBLG rods were packed in an interdigitated manner in their respective domains. Some areas in Figure 7d showed a 6-fold symmetry, although the cylinders did not pack in a perfect hexagonal lattice throughout the whole domain. The lack of a high order in the microstructures shown in the TEM micrographs might also be attributed to the rigidity and the low chain mobility of the PMPCS and PBLG rods. However, to the best of our knowledge, no similar morphology (hexagonally packed cylinders with hexagonally packed helices, which can be called hexagon in cylinder) has been observed in rod-rod BCP systems.

2D WAXD patterns of the samples with X-ray beam along *X* (shear direction), *Y*, and *Z* directions are shown in Figure 7f–h, respectively. In parts f and g of Figure 7, a pair of strong diffraction arcs could be observed on the meridian in the low-angle region, in which the reflection from the Φ_N phase of PMPCS was embedded in the first-order reflection of the Φ_H phase of PBLG, and higher-order reflections from the hexagonal columnar arrangement of PBLG were visible in Figure 7f. A ring pattern at low angles could be observed in Figure 7h with X-ray beam along the *X* direction, indicating polydomain nature of the hexagonal arrangement of PBLG in the direction

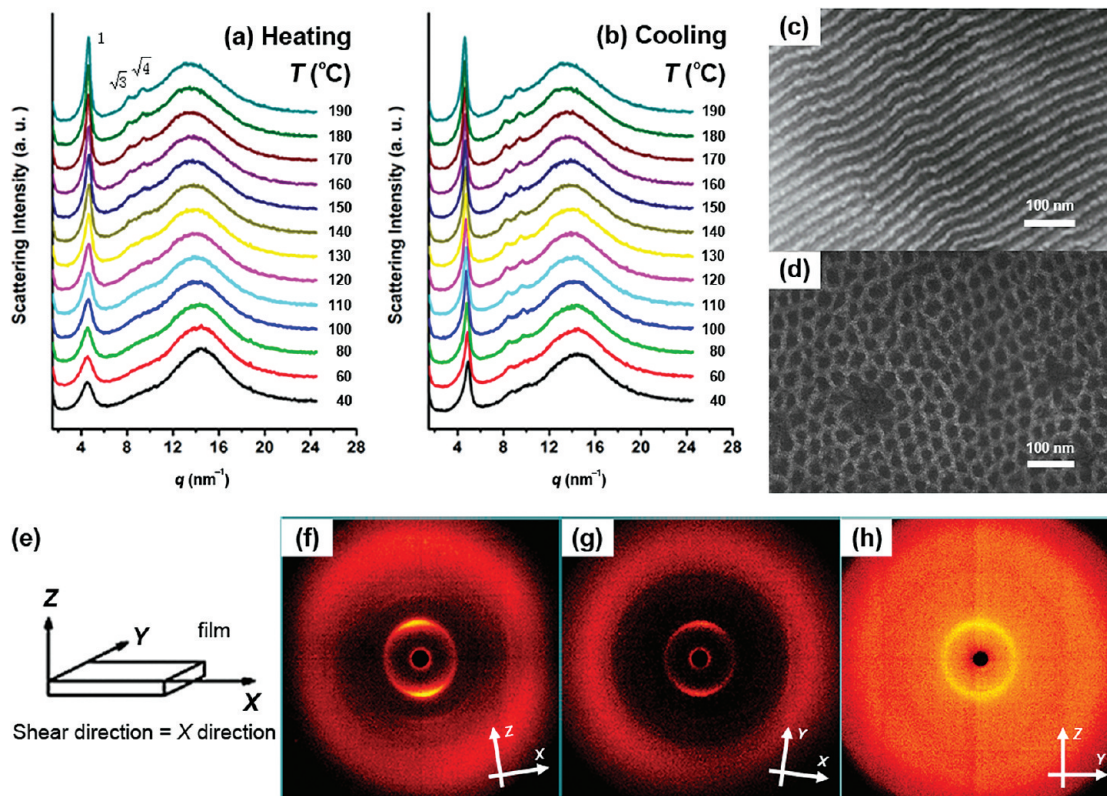


Figure 7. 1D WAXD powder patterns of PMPCS₄₂-*b*-PBLG₁₇₃ during first heating (a) and cooling (b) experiments. TEM micrographs of ultramicrotomed films of PMPCS₄₂-*b*-PBLG₁₇₃ (c and d). Schematic drawing of the shearing geometry with *X*-axis the shear direction (e). 2D WAXD patterns of a sheared film sample of PMPCS₄₂-*b*-PBLG₁₇₃ with *X*-ray beam along *Y* (f), *Z* (g), and *X* (h) directions.

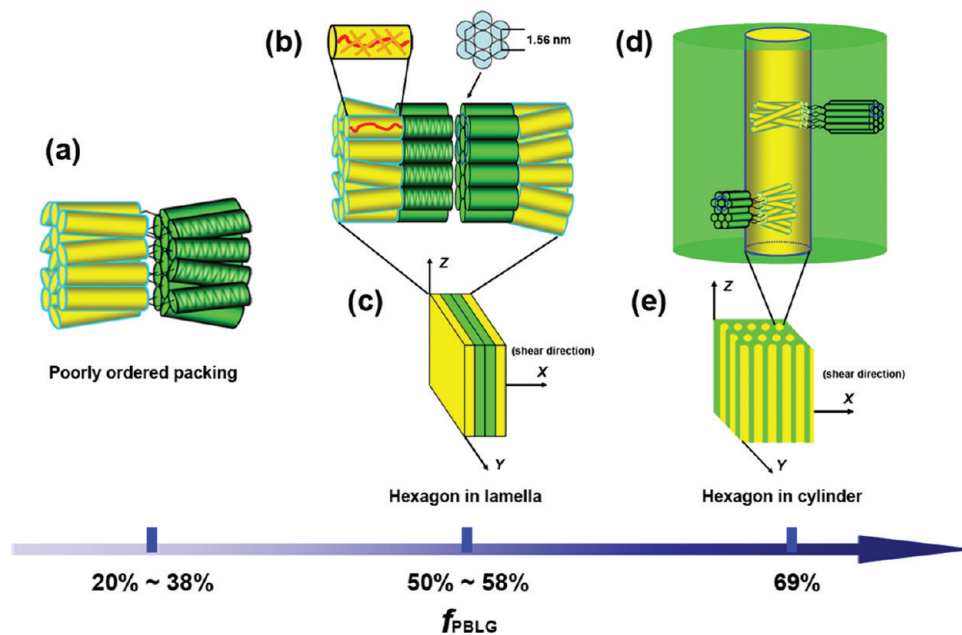


Figure 8. Schematic representation of the proposed model for the self-assembly of the rod-rod diblock copolymer in poorly ordered packing (a), hexagon in lamella (b), and cylinder (d) structures, respectively. Schematic drawings of the shearing geometry with the *X*-axis being the shear direction (c and e).

perpendicular to the shear direction. These results also indicated that after mechanical shearing the PMPCS rods and the PBLG rods were both aligned parallel to the shear direction (*X* direction). Therefore, according to the TEM micrographs and the 2D WAXD patterns, the mechanical shearing forced the orientation of the self-assembling morphology,⁵³ with the

polymer backbones aligned along the shear direction and the cylinders of the microstructure perpendicular to the shear direction. However, the development of the cylinder morphology suggested that the alignment of the rods along the shear direction was far from perfect, which is evident from Figure 7g. A schematic representation is shown in Figure 8 which exhibits

different hierarchical self-assembling structures of the copolymers with different volume fractions of PBLG. In summary, the copolymer with a low volume fraction of PBLG adopted a poorly ordered packing, in which the detailed packing schemes of the PMPCS and PBLG rods were unclear, although a bilayer-type packing was drawn in Figure 8 for the ease of drawing. With the increase in f_{PBLG} , the morphology transformed first into a stacked bilayer structure in an HL morphology, and then into a hexagon in cylinder morphology with the PMPCS domain as cylinders and the PBLG domain as the matrix at the relatively high content of the PBLG block.

It will be more interesting to know how the self-assembling structure changes when the two rods in the rod-rod BCPs have more different diameters. The additional benefit of using rods with more different diameters is the clear separation of characteristic reflections from each rod in WAXD patterns, which facilitates easier structural analysis. On the other hand, the larger difference in the area of projection along the long axis of the rods will affect the curvature of the microphase-separated structure. To this end, further research is currently underway.

Conclusions

In this study, alkyne and azido functionalities were introduced as termination groups in both PMPCS and PBLG homopolymers by utilizing α -functionalized initiators for copper-mediated ATRP of 2,5-bis[(4-methoxyphenyl)oxycarbonyl]styrene and ROP of γ -benzyl-L-glutamate *N*-carboxyanhydride. Block copolymers were subsequently synthesized by the Huisgen's 1,3-dipolar cycloaddition (click chemistry) from homopolymers possessing azide and alkyne functionalities. The click coupling reaction was proven to be facile and efficient based on GPC, NMR, and FTIR analyses. A hexagon in lamella structure was proposed based on the 1D WAXD, 2D WAXD, and TEM analyses for BCPs with f_{PBLG} of ~ 0.50 . And the PMPCS blocks were considered to be packed in a columnar nematic phase, while PBLG segments had a tightly packed, hexagonal arrangement of α -helices. According to the TEM observation and simulation of the molecular lengths of the copolymers, a stacked bilayer structure in the HL morphology was proposed to describe the nanoscale microphase-separated structure of these copolymers. By increasing f_{PBLG} to ~ 0.69 , a microphase-separated hexagon in cylinder morphology was observed, in which PMPCS formed the core of the cylinders surrounded by PBLG in the Φ_{H} phase and both rods were packed in an interdigitated manner in their own domains. Results from TEM observation and 2D WAXD patterns of the copolymers indicated that the development of the LC phases did not destroy the self-assembling structures from microphase separation. This work also confirms that both MJLCPs and polypeptides obtained from controlled polymerization methods are excellent rod-like building blocks to form rod-rod BCPs with nanoscale hierarchical structures.

Acknowledgment. This research was supported by the National Natural Science Foundation of China (Grant Nos.: 20634010 and 20874003).

Supporting Information Available: Text discussing and figure showing the FTIR spectra of the azido-PBLG₁₉ homopolymer and PMPCS-*b*-PBLG BCPs. This material is available free of charge via the Internet at <http://pubs.acs.org>.

References and Notes

- Bates, F. S. *Science* **1991**, *251*, 898–905.
- Fredrickson, G. H.; Bates, F. S. *Annu. Rev. Mater. Sci.* **1996**, *26*, 501–550.
- Leibler, L.; Orland, H.; Wheeler, J. C. *J. Chem. Phys.* **1983**, *79*, 3550–3557.
- Ciferri, A., *Supramolecular Polymers*; Marcel Dekker: New York, 2000.
- Bates, F. S.; Schulz, M. F.; Rosedale, J. H.; Almdal, K. *Macromolecules* **1992**, *25*, 5547–5550.
- Singh, C.; Goulian, M.; Liu, A. J.; Fredrickson, G. H. *Macromolecules* **1994**, *27*, 2974–2986.
- Matsen, M. W. *J. Chem. Phys.* **1996**, *104*, 7758–7764.
- Jenekhe, S. A.; Chen, X. L. *Science* **1999**, *283*, 372–375.
- Klok, H.-A.; Lecommandoux, S. *Adv. Mater.* **2001**, *13*, 1217–1229.
- Stupp, S. I.; LeBonheur, V.; Walker, K.; Li, L. S.; Huggins, K. E.; Keser, M.; Amstutz, A. *Science* **1997**, *276*, 384–389.
- Zhang, Y.; Tajima, K.; Hirota, K.; Hashimoto, K. *J. Am. Chem. Soc.* **2008**, *130*, 7812–7813.
- Wang, H. H.; Wang, H. H.; Urban, V. S.; Littrell, K. C.; Thiagarajan, P.; Yu, L. *J. Am. Chem. Soc.* **2000**, *122*, 6855–6861.
- Scherf, U.; Adamczyk, S.; Gutacker, A.; Koenen, N. *Macromol. Rapid Commun.* **2009**, *30*, 1059–1065.
- Cha, J. N.; Stucky, G. D.; Morse, D. E.; Deming, T. J. *Nature* **2000**, *403*, 289–292.
- Deming, T. J. *Macromolecules* **1999**, *32*, 4500–4502.
- Nowak, A. P.; Breedveld, V.; Pakstis, L.; Ozbas, B.; Pine, D. J.; Pochan, D.; Deming, T. J. *Nature* **2002**, *417*, 424–428.
- Bellomo, E. G.; Wyrsta, M. D.; Pakstis, L.; Pochan, D. J.; Deming, T. J. *Nat. Mater.* **2004**, *3*, 244–248.
- Rodriguez-Hernandez, J.; Lecommandoux, S. *J. Am. Chem. Soc.* **2005**, *127*, 2026–2027.
- Rao, J.; Zhang, Y.; Zhang, J.; Liu, S. *Biomacromolecules* **2008**, *9*, 2586–2593.
- Kros, A.; Jesse, W.; Metselaar, G. A.; Cornelissen, J. J. L. M. *Angew. Chem., Int. Ed. Engl.* **2005**, *44*, 4349–4352.
- Papadopoulos, P.; Floudas, G.; Schnell, I.; Aliferis, T.; Iatrou, H.; Hadjichristidis, N. *Biomacromolecules* **2005**, *6*, 2352–2361.
- Sanchez-Ferrer, A.; Mezzenga, R. *Macromolecules* **2009**, *43*, 1093–1100.
- Kong, X.; Jenekhe, S. A. *Macromolecules* **2004**, *37*, 8180–8183.
- Zhou, Q.-F.; Li, H.-M.; Feng, X.-D. *Macromolecules* **1987**, *20*, 233–234.
- Zhou, Q.-F.; Zhu, X.; Wen, Z. *Macromolecules* **1989**, *22*, 491–493.
- Xu, G.; Wu, W.; Shen, D.; Hou, J.; Zhang, S.; Xu, M.; Zhou, Q. *Polymer* **1993**, *34*, 1818–1822.
- Chen, X.-F.; Shen, Z.; Wan, X.-H.; Fan, X.-H.; Chen, E.-Q.; Ma, Y.; Zhou, Q.-F. *Chem. Soc. Rev.* **2010**, DOI:10.1039/b814540g.
- Li, C. Y.; Tenneti, K. K.; Zhang, D.; Zhang, H.; Wan, X.; Chen, E.-Q.; Zhou, Q.-F.; Carlos, A.-O.; Igos, S.; Hsiao, B. S. *Macromolecules* **2004**, *37*, 2854–2860.
- Tenneti, K. K.; Chen, X.; Li, C. Y.; Tu, Y.; Wan, X.; Zhou, Q.-F.; Sics, I.; Hsiao, B. S. *J. Am. Chem. Soc.* **2005**, *127*, 15481–15490.
- Tu, Y.; Wan, X.; Zhang, D.; Zhou, Q.; Wu, C. *J. Am. Chem. Soc.* **2000**, *122*, 10201–10205.
- Xie, H.-L.; Liu, Y.-X.; Zhong, G.-Q.; Zhang, H.-L.; Chen, E.-Q.; Zhou, Q.-F. *Macromolecules* **2009**, *42*, 8774–8780.
- Zhang, J.; Cao, H.; Wan, X.; Zhou, Q. *Langmuir* **2006**, *22*, 6587–6592.
- Lecommandoux, S.; Achard, M.-F.; Langenwalter, J. F.; Klok, H.-A. *Macromolecules* **2001**, *34*, 9100–9111.
- Lee, H.-F.; Sheu, H.-S.; Jeng, U. S.; Huang, C.-F.; Chang, F.-C. *Macromolecules* **2005**, *38*, 6551–6558.
- Babin, J.; Taton, D.; Brinkmann, M.; Lecommandoux, S. *Macromolecules* **2008**, *41*, 1384–1392.
- Ho, C.-C.; Lee, Y.-H.; Dai, C.-A.; Segalman, R. A.; Su, W.-F. *Macromolecules* **2009**, *42*, 4208–4219.
- Li, C.; Ge, Z.; Fang, J.; Liu, S. *Macromolecules* **2009**, *42*, 2916–2924.
- Agut, W.; Taton, D.; Lecommandoux, S. *Macromolecules* **2007**, *40*, 5653–5661.
- Zhang, D.; Liu, Y.-X.; Wan, X.-H.; Zhou, Q.-F. *Macromolecules* **1999**, *32*, 5183–5185.
- Poché, D. S.; Moore, M. J.; Bowles, J. L. *Synth. Commun.* **1999**, *29*, 843–854.
- Pyzdek, W. *Macromolecules* **1980**, *13*, 153–157.
- Ye, C.; Zhang, H.-L.; Huang, Y.; Chen, E.-Q.; Lu, Y.; Shen, D.; Wan, X.-H.; Shen, Z.; Cheng, S. Z. D.; Zhou, Q.-F. *Macromolecules* **2004**, *37*, 7188–7196.
- Laurent, B. A.; Grayson, S. M. *J. Am. Chem. Soc.* **2006**, *128*, 4238–4239.

- (44) Huisgen, R. In *1,3-Dipolar Cycloaddition Chemistry*; Padwa, A., Ed.; Wiley: New York, 1984; pp 1–176.
- (45) Blout, E. R.; Asadourian, A. *J. Am. Chem. Soc.* **1956**, *78*, 955–961.
- (46) Lee, N. H.; Frank, C. W. *Langmuir* **2003**, *19*, 1295–1303.
- (47) Papadopoulos, P.; Floudas, G.; Klok, H. A.; Schnell, I.; Pakula, T. *Biomacromolecules* **2004**, *5*, 81–91.
- (48) Pragliola, S.; Ober, C. K.; Mather, P. T.; Jeon, H. G. *Macromol. Chem. Phys.* **1999**, *200*, 2338–2344.
- (49) Gallot, B. *Prog. Polym. Sci.* **1996**, *21*, 1035–1088.
- (50) Watanabe, J.; Uematsu, I. *Polymer* **1984**, *25*, 1711–1717.
- (51) Ibarboure, E.; Rodriguez-Hernandez, J.; Papon, E. *J. Polym. Sci., Part A: Polym. Chem.* **2006**, *44*, 4668–4679.
- (52) Gao, L.-C.; Zhang, C.-L.; Liu, X.; Fan, X.-H.; Wu, Y.-X.; Chen, X.-F.; Shen, Z.; Zhou, Q.-F. *Soft Matter* **2008**, *4*, 1230–1236.
- (53) Tennesi, K. K.; Chen, X.; Li, C. Y.; Wan, X.; Fan, X.; Zhou, Q.-F.; Rong, L.; Hsiao, B. S. *Soft Matter* **2008**, *4*, 458–461.